

2010

Efficient Cooling in Cylinder Heads for Air Brake Compressors

Andreas Brandl

Hoerbiger Ventilwerke GmbH & Co. KG

Follow this and additional works at: <https://docs.lib.purdue.edu/icec>

Brandl, Andreas, "Efficient Cooling in Cylinder Heads for Air Brake Compressors" (2010). *International Compressor Engineering Conference*. Paper 1987.

<https://docs.lib.purdue.edu/icec/1987>

This document has been made available through Purdue e-Pubs, a service of the Purdue University Libraries. Please contact epubs@purdue.edu for additional information.

Complete proceedings may be acquired in print and on CD-ROM directly from the Ray W. Herrick Laboratories at <https://engineering.purdue.edu/Herrick/Events/orderlit.html>

Efficient Cooling in Cylinder Heads for Air Brake Compressors

International Compressor Engineering Conference at Purdue 2010

Andreas BRANDL

HOERBIGER Ventilwerke GmbH & Co KG,
Braunhubergasse 23, 1110 Vienna, Austria
E-mail: andreas.brandl@hoerbiger.com

ABSTRACT

The high compression ratio in air brake compressors leads to very elevated gas temperatures at the discharge side of the cylinder head. An unsteady 1-D model of the gas flow through compressor and cylinder head has been developed in order to investigate the cooling performance and the energetic efficiency of different channel designs in combination with certain plenum sizes. A prototype cylinder head was set up following guidelines worked out with the help of this simulation tool. The present work describes the unsteady 1-D model with its assumptions and simplifications, a step by step dimensioning of the plenum volumes and channels in the cylinder head by applying the simulation model on a given compressor in order to obtain an ideal cylinder head design. Finally, a selection of measurements is presented and compared to the results of the simulation.

1. INTRODUCTION

The cylinder head is a crucial part of the air brake compressor. Suction, discharge and coolant channels have to be arranged within very limited space. The cylinder head incorporates suction and discharge valves (usually reed valves) as well as an optional energy saving system to reduce energy consumption at idle running (for air brake compressors that are directly connected to the drive system of the vehicle). The air brake compressor takes the suction gas at ambient pressure and temperature and discharges in a vessel with e.g. 12.5 bars. Due to the high maximum speed of 3500 rpm, the peak pressures in the cylinder can increase substantially, if cylinder head and valve design are not dimensioned accordingly. This compression ratio would lead to extremely high gas temperatures, oil cracking and in succession to valve failure as well as to a failure of the pneumatic components downstream the cylinder head. Even if the pressure losses at the discharge side are minimized, compression ratios of higher than 12 emerge. Depending on the ambient conditions and on the heat transfer situation in the cylinder, this results in discharge gas temperatures of up to 400°C. The aim is to cool down the discharge gas within the cylinder head in an optimal way. Current cylinder heads often discharge at temperatures above 250°C. This eventually requires tubing outside the cylinder head to cool down the gas before feeding it into the pneumatic system of the vehicle. Generating a high heat transfer coefficient from discharge gas to the head material is one necessary step towards ideal cooling. Enhancing the heat transfer from gas to solid boosts the head material temperature if no special care is taken. Die cast aluminum for instance, has a relatively low temperature limit that should not be exceeded. If material temperatures rise above 200°C, the latter risks to suffer damage due to compressed gas imprisoned in the material as a result of the die casting process. To summarize, temperature and energy management in the cylinder head are of utmost importance.

2. COMPRESSOR MODELING

Compressor and cylinder head are modeled by a succession of different basic elements. Chambers of constant volume, like suction or discharge plenum chamber, as well as chambers of variable volume, like the cylinder, are modeled in a 0-D approach. All state variables are time dependent but constant throughout the chamber domain. The chambers are connected by valves, orifice elements or channel elements. Valves are treated as ideal valves, which means that they can take only two states, completely open or entirely closed. As soon as the upstream pressure exceeds the downstream pressure they immediately make the full flow area accessible. The motion of the reed valve

is not incorporated. Channels are accounted for by an unsteady compressible 1-D pipe flow approach. Heat transfer as well as wall friction is included in the 1-D model.

2.1 Valve and Orifice Elements

The mass flow through valves and orifices, see figure 1, is assumed to be quasi – steady and is given by Saint Venant and Wantzel (Spurk, 1996). Velocities are assumed to be zero in the chambers upstream and downstream the restriction. The apertures are assumed to be large enough and the pressure ratios over the orifices small enough for the Mach number in the orifice to stay below 1. The ideal valves as well as the orifices are accounted for by their effective flow areas, which have to be determined empirically or by means of a CFD analysis.

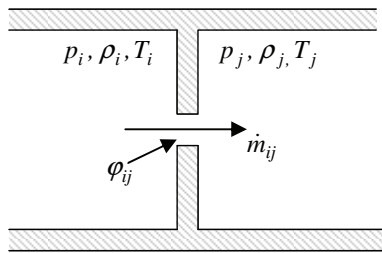


Figure 1: Orifice between chambers *i* and *j*.

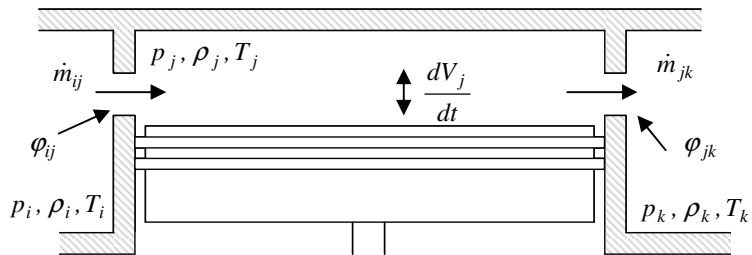


Figure 2: Chamber element *j* with adjacent chambers *i* and *k*.

2.2 Chamber Elements

For a given piston motion and thus a given rate of change of volume, see figure 2, the governing equations for chamber *j* are found by applying continuity equation, energy balance and equation of state for an ideal gas to the chamber. It is assumed that except for the piston work there is no other work done on the chamber and that the chamber is thermally insulated. Furthermore the inflow and outflow processes are assumed to be quasi – steady. For mass flows as indicated in figure 2, the governing equations for the chamber element become,

$$\frac{d\rho_j}{dt} = \frac{\dot{m}_{ij} - \dot{m}_{jk}}{V_j} - \frac{\rho_j}{V_j} \frac{dV_j}{dt}, \tag{1}$$

$$\frac{dp_j}{dt} = -\kappa \frac{p_j}{V_j} \frac{dV_j}{dt} + \kappa \frac{p_i}{\rho_i V_j} \dot{m}_{ij} - \kappa \frac{p_j}{\rho_j V_j} \dot{m}_{jk}. \tag{2}$$

Together with the mass flow relation of St. Venant, the thermal and the caloric equation of state for ideal gases, the equations (1) and (2) provide the tools to determine the thermodynamic change of state of the chamber element.

2.3 Channel Elements

A channel element is characterized by its length *L*, the cross sectional area *A* and perimeter *P*. The flow area of the channels is assumed to be large enough for the pressure ratio to stay small enough in order to avoid choked flow. The frictional effects are incorporated by introducing a friction factor for coiled tubes. The channel length is significant for high heat removal. A bent channel permits higher channel lengths in the cylinder head. The relations for the friction factor for coiled tubes (*d_h* is the hydraulic diameter of the tube and *D* the diameter of the coil) and for the heat transfer coefficient are given by (Verein Deutscher Ingenieure, 1984),

$$\xi_w = \frac{0.3164}{Re^{0.25}} \left[1 + 0.095 \left(\frac{d_h}{D} \right)^{0.5} Re^{0.25} \right], \tag{3}$$

$$\tau_w = \frac{\xi_w \rho v^2}{4}; \tag{4}$$

The heat transfer to the surrounding material is accounted for, by an overall heat transfer coefficient, implicitly for turbulent pipe flow from gas to solid (Verein Deutscher Ingenieure, 1984),

$$\alpha_{gas} = \frac{Nu\lambda_{gas}}{d_h}, \tag{5}$$

$$Nu = \frac{\xi_{Nu}(Re-1000)Pr}{8} \left[1 + \left(\frac{d_h}{L} \right)^{\frac{2}{3}} \right], \tag{6}$$

$$1 + 12.7 \sqrt{\frac{\xi_{Nu}}{8}} \left(Pr^{\frac{2}{3}} - 1 \right)$$

$$\xi_{Nu} = (1.82 \log_{10}(Re) - 1.64)^{-2}. \tag{7}$$

The overall heat transfer coefficient α_{ov} is identified as the reciprocal of the sum of the individual thermal resistances (Incropera, 1996). Next to the heat transfer from gas to solid, heat conduction in the material that is separating gas and coolant flow ($\lambda_{solid} = 120W/(mK)$, $l_{solid} = 1cm$) and heat transfer from solid to coolant (water, $\alpha_{water} = 6000W/(m^2K)$) is considered. The coolant mass flow is assumed to be high enough that, in combination with the large specific heat capacity of water (compared to air), the temperature increase of the coolant in the cylinder head is very moderate compared to the temperature change of the gas. In consideration of this fact, the coolant is assumed to be at a constant temperature of $T_{water}=110^\circ C$.

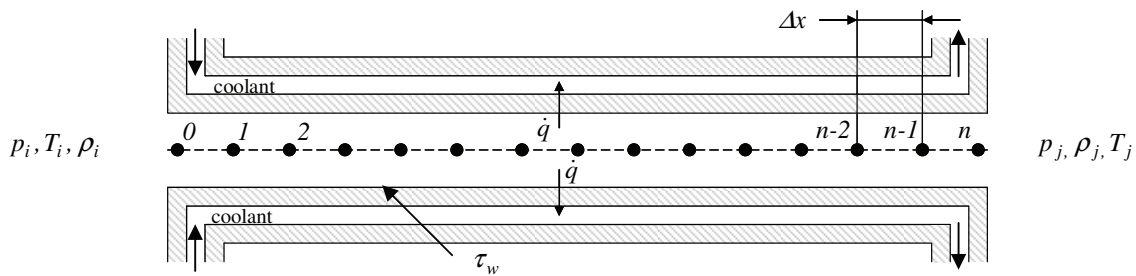


Figure 3: Channel element with adjacent chambers i and j.

The governing equations for the one dimensional, unsteady, compressible pipe flow are obtained by applying mass-, momentum-, and energy balance to an infinitesimal volume, giving

$$\frac{\partial(\rho A)}{\partial t} + \frac{\partial(\rho v A)}{\partial x} = 0, \tag{8}$$

$$\frac{\partial(\rho v A)}{\partial t} + \frac{\partial(\rho v^2 A + p A)}{\partial x} = p \frac{\partial A}{\partial x} - A \frac{\xi_w}{d_h} \frac{\rho v^2}{2} \frac{v}{|v|}, \tag{9}$$

$$\frac{\partial \left(\rho A \left(c_v T + \frac{v^2}{2} \right) \right)}{\partial t} + \frac{\partial \left(\rho v A \left(c_v T + \frac{v^2}{2} \right) + A v p \right)}{\partial x} = \alpha_{ov} (T_{water} - T) P. \tag{10}$$

For numerical reasons it is favorable to solve the governing equations in conservation form, as presented in equations (8), (9) and (10). Instead of solving directly for pressure p , temperature T , etc, the problem is solved for ρA , $\rho v A$ and $\rho A(c_v T + v^2/2)$ to avoid numerical instabilities and oscillations in the results. At the inflow boundary condition, point 0 in figure 3, pressure and temperature (and thus the density) are fixed, assuming isentropic acceleration starting from the plenum chamber i upstream the channel. The velocity is extrapolated from grid point 1 and 2. Assuming subsonic outflow conditions at point n , the pressure at the channel outflow can be set equal to the pressure of the chamber downstream the channel. Temperature and velocity are extrapolated from grid points $n-1$ and $n-2$ and the density is then determined by means of the ideal gas law. Each time step has to be determined such that the numerical integration remains stable. The CFL condition can serve as a stability criterion (Anderson 1995).

The equations are discretized and solved, using MacCormack’s technique, an explicit predictor - corrector method (Anderson, 1995).

2.4 Composition of cylinder head model

The cylinder head is modeled as a succession of basic elements described in the previous chapters. Suction gas enters from constant suction condition (p_{amb}, T_{amb}) through the orifice ϕ_{in} into the suction chamber of volume V_{suc} . The suction valve is represented by the orifice ϕ_{suc} . The cylinder is modeled as a chamber element of variable volume that discharges through the ideal discharge valve ϕ_{dis} into the discharge chamber V_{dis} . The connection between discharge chamber and pressure vessel is provided by the discharge channel element of length L , cross sectional area A and cross section perimeter P and the exit chamber with exit orifice.

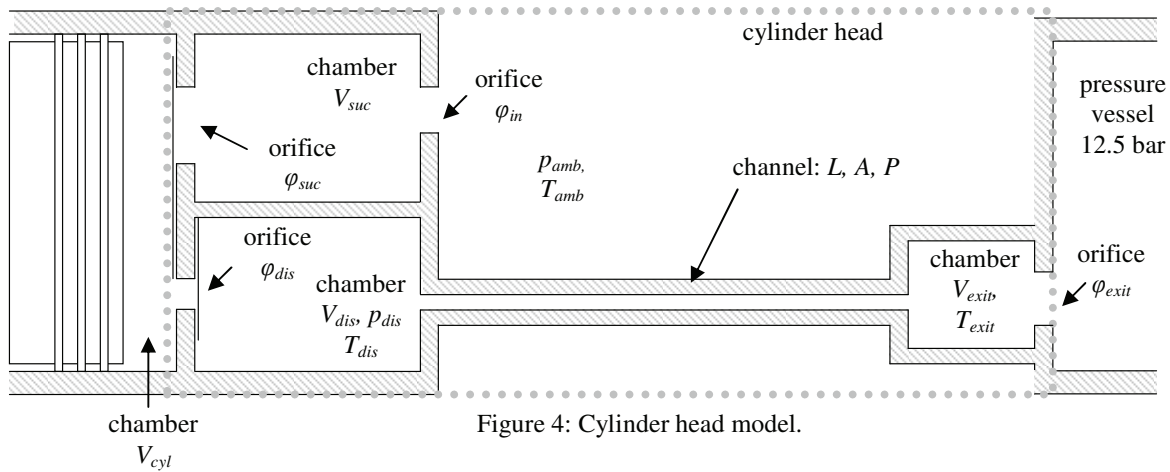


Figure 4: Cylinder head model.

3. APPLICATION ON A GIVEN COMPRESSOR

The model of the compressor and the cylinder head described in chapter 2 is now used to determine the composition of an efficient cylinder head for a 400cm³ air brake compressor. Suction pressure is 1bar, suction temperature is fixed to 70°C to account for the heating up of the suction gas as it passes the suction side of the cylinder head. Measurements have shown that 70°C at the suction valve is a reasonable value. The pressure in the vessel is set to 12.5 bars. Speed varies between 500rpm and 3500rpm. To dimension the head assembly, a speed of 3000rpm is chosen, assuming that for lower speeds the specific power consumption (average power consumption referred to average mass flow) and discharge temperatures will diminish. The valve system has been designed according to state of the art knowledge. Maximum effective flow area of the chosen suction valve is 4.5cm² and 1.7cm² for the discharge valve. The resulting clearance volume is about 11cm³, corresponding to 2.7%. A major heat exchange usually implicates a high pressure loss and thus high power consumption. An energy efficient design requires a big amount of space which is not always available. In order to find an optimal compromise between exit gas temperature, power consumption, mass flow and occupied space, selected parameters will be permutated while the rest remains at constant initial dimensions, see table 1.

Table 1: Dimensions of the initial arrangement used for permuting the parameters.

ϕ_{in}	V_{suc}	V_{dis}	L	A	P	V_{exit}	ϕ_{exit}
4cm ²	75cm ³	190cm ³	0.33m	80mm ²	82mm	20cm ³	1.9cm ²

The values for mass flow, specific power consumption and temperature that will be presented in chapters 3.1 and 3.2 are mean values, averaged over the last calculated compression period,

$$\dot{m}_{av} = \sum_t \dot{m}_t \Delta t_t n, \tag{11}$$

$$\dot{w}_{av} = -\frac{1}{\dot{m}_{av}} \sum_t p_{cyl,t} \left(\frac{dV_{cyl}}{dt} \right)_t \Delta t_t n, \tag{12}$$

$$T_{av} = \frac{1}{\dot{m}_{av} c_p} \sum_t \dot{m}_t \left(c_p T_t + \frac{v_t^2}{2} \right) \Delta t_t n. \tag{13}$$

3.1 Suction side

The suction side (suction inlet and suction chamber) has a big influence on mass flow, power consumption and discharge temperature T_{dis} . The simulation has been run for different values of inlet orifice flow area ϕ_{in} and suction chamber volume V_{suc} . The rest of the parameters were kept constant, according to table 1. Figure 5 shows the mass flow for $V_{suc} = 100\text{cm}^3$. For ϕ_{in} bigger than 2cm^2 , the mass flow does not change considerably with the suction volume (assuming reasonable suction volume values), for this reason the mass flow is represented for one suction volume only. From that mass flow characteristic it can be concluded that the inlet orifice should not be smaller than 4cm^2 in order not to lose too much mass flow. Furthermore figure 5 shows that the suction volume does not have too much influence on the power consumption for ϕ_{in} bigger than 4cm^2 . Summing up, the inlet orifice for the given compressor and valve arrangement at a speed of 3000rpm should be at least 4cm^2 to obtain reasonable values for mass flow, power consumption and discharge temperature.

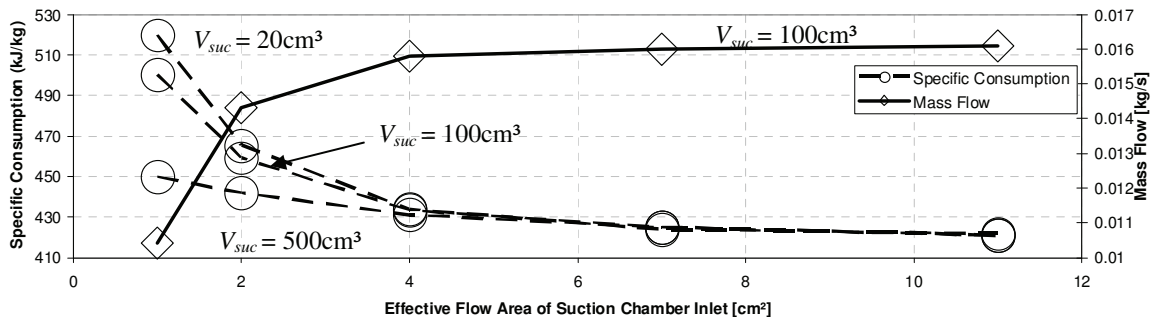


Figure 5: \dot{w} and \dot{m} for different values of suction chamber inlet ϕ_{in} and suction chamber volume V_{suc} .

For small inlet orifices the discharge temperature T_{dis} rises considerably, which is critical with respect to oil cracking. The exit temperature T_{exit} , however, is not influenced as much as the discharge temperature. The mass flow reduction that comes along with small inlet orifices makes it easier to cool the gas down. A small suction filter upstream the inlet orifice would have similar effects like a small inlet orifice.

3.2 Discharge side

The discharge side, comprising the discharge chamber and the discharge channel, has a strong impact on power consumption and exit temperature T_{exit} . Shape and size of the discharge channel control the exit temperature. The discharge volume and the cross sectional area of discharge channel strongly influence the discharge pressure and thus the energy consumption. Figure 6 shows the specific power consumption and exit temperature T_{exit} for different values of discharge volume V_{dis} and flow area of the discharge channel A .

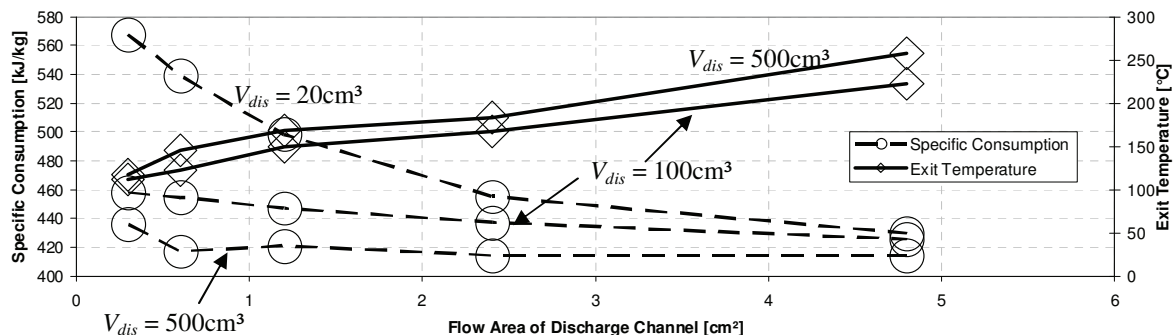


Figure 6: \dot{w} and T_{exit} for different values of discharge channel flow area A and discharge chamber volume V_{dis} .

Even for large flow areas the discharge volume V_{dis} has a noticeable effect on the specific power consumption. Reducing the discharge channel flow area while keeping the cross section perimeter constant reduces the hydraulic diameter of the channel and effects the Reynolds and Nusselt number in the channel, which has large influences on friction and heat transfer. Figure 6 shows that a reduction of the flow area results in a sufficiently efficient heat transfer coefficient for reducing the exit temperature T_{exit} , even though the pressure loss and thus the discharge temperature T_{dis} increase. For the given arrangement and fixed cross sectional perimeter P , low exit temperatures require relatively small discharge pipe flow areas and small hydraulic diameters. In order to obtain satisfying exit temperatures at reasonable power consumption, the discharge volume has to be maximized according to figure 6. The low power consumption for $V_{dis}=500\text{cm}^3$ and $A=0.6\text{cm}^2$ in figure 6 issues from favorable flow dynamics in the discharge pipe. The pressure in the discharge chamber is at a minimum by the time the discharge valve opens.

For small values of discharge volume and discharge channel flow area, the mass flow develops a rather strong dependency on these quantities, see figure 7. Mass flow decreases if the discharge and thus the cylinder pressure have not balanced with vessel pressure by the time the valve closes. Due to higher pressure and thus higher density, a higher amount of mass remains in the clearance volume. With small discharge pipe flow areas the discharge pressure at valve closing time is extremely high for small discharge volumes, hence there is a huge loss in mass flow. For larger pipe sections the discharge pressure decreases much faster at small discharge volumes and this results in elevated mass flow. The diminishing mass flow at high flow areas for $V_{dis} = 20\text{cm}^3$ is again due to dynamic effects in the discharge chamber, channel and exit chamber for this special arrangement, but does not reflect a general trend.

Summing up, for low exit temperatures the cross sectional area of the discharge pipe has to be dimensioned sufficiently small (for the given cross sectional perimeter), according to figure 6. To avoid excessive energy losses (figure 6) and mass flow losses (figure 7), the discharge volume has to be chosen sufficiently large.

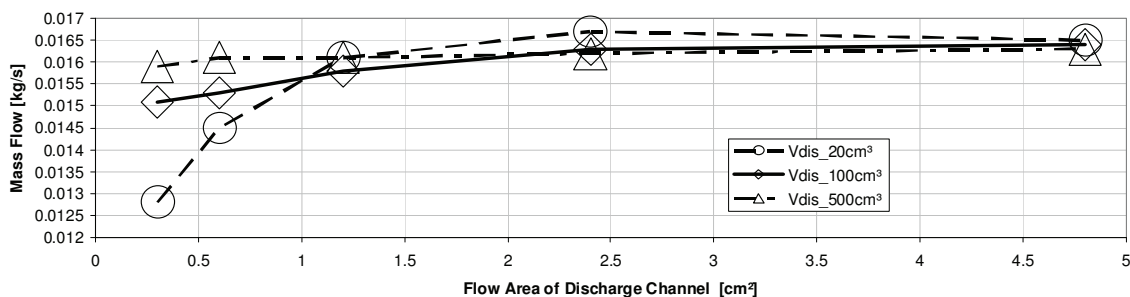


Figure 7: Mass flow for different values of discharge channel flow area A and discharge volume V_{dis} .

3.3 Setting up the dimensions

With the help of a CAD system and the findings of chapter 3.1 and 3.2, a cylinder head consisting of chambers, orifices and channels (according to figure 4), with incorporated energy saving system (additional, connectible clearance that is connected to the cylinder volume during idling) has been designed with regard to production and sealing technology, etc. The geometry that was used as initial arrangement for simulation, see table 1, proves to be an adequate compromise in terms of performance and efficiency and was thus implemented in the prototype cylinder head.

4. COMPARISON WITH MEASUREMENTS

A prototype cylinder head was adapted in order to fit on an existing cylinder block. The assembly was in-house tested to verify the promising results of the preceding preliminary design. The tests were run from ambient suction condition to a discharge pressure of 12.5bars.

4.1 Pressure course in discharge chamber

Figure 8 shows the course of discharge pressure for measurement and calculation. There are four main differences between both curves. At the valve opening event the pressure rises much faster in the measurement. This is quite probably due to retarded opening of the real valve compared to the ideal valve that was used in the calculation. Also

peak pressures differ from each other. In the measurements, the mass flow rises first linearly with compressor speed and, for some reason, falls then at higher speeds behind the linear characteristic. With the present compressor model this behavior, which might be the reason for the higher peak pressures in the calculation, cannot be reproduced. The third main difference is the periodic time of the pressure oscillation in the discharge chamber. The calculated pressure oscillates at a higher frequency. One reason for that might be the higher natural frequency of the gas movement in the discharge channel at higher temperatures and thus at higher sonic speeds. Measurements reveal that the temperature in the discharge chamber is considerably lower than in the calculation where isentropic compression and adiabatic chambers were assumed. Another difference could be due to frictional effects. The amplitude of the oscillation is too high in the calculation. The relation for the friction coefficient, equation (3), holds for smooth pipes. Turbulent pipe flow is very sensitive to wall roughness and results in higher friction coefficients, which might partially explain the raised amplitudes of the pressure oscillations.

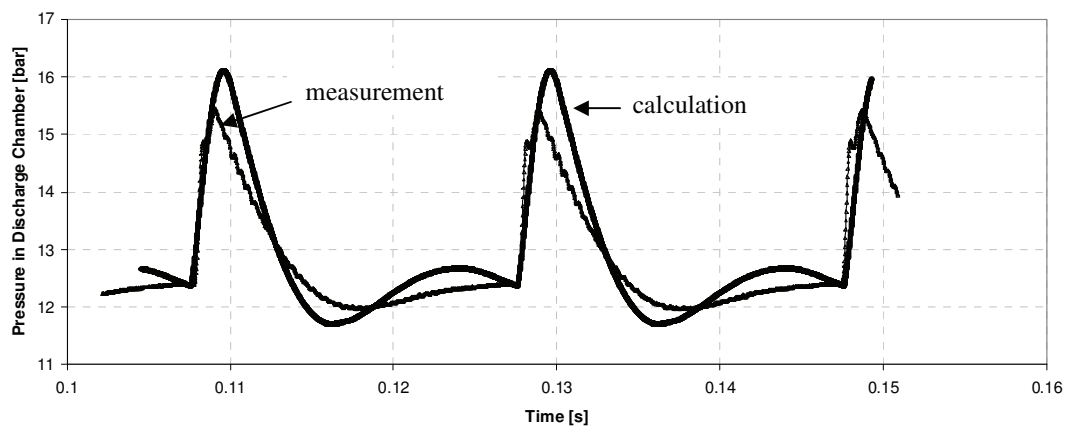


Figure 8: Pressure in discharge chamber. Comparison between measurement and calculation at 3000rpm.

4.3 Mean temperature in exit chamber

Figure 9 reveals that the measured exit temperatures are 30°C to 40°C lower than the calculated ones. One reason for the comparatively big discrepancy is that heat transfer is only included in the discharge channel. Since the valve plate that is covering the cylinder is cooled, the heat transfer in the cylinder might be quite important as well.

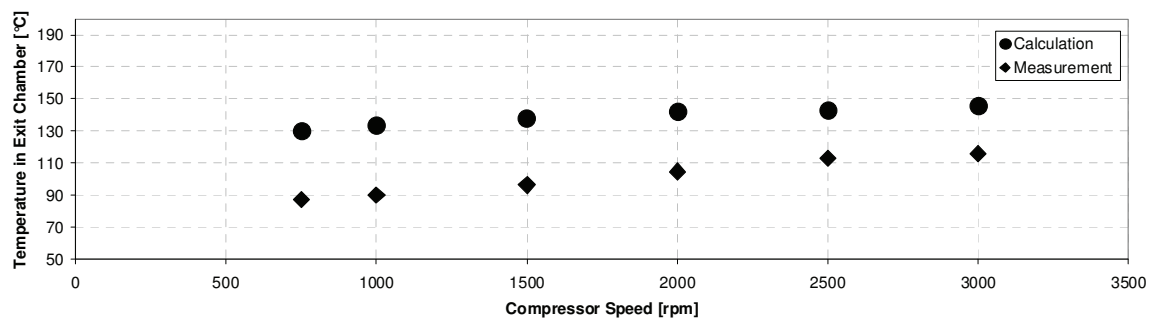


Figure 9: Exit temperature T_{exit} for measurement and calculation.

In the same manner, the discharge chamber is configured in a way that allows high values for the heat transfer coefficient. Finding reliable heat transfer correlations for the cylinder and for the flow in the discharge chamber is a rather delicate matter and has been neglected for this study. The measurements were accomplished with a constant inflow coolant temperature of 80°C. The experiments show that the temperature increase of the cooling water is about 5°C at low speeds and around 20°C for high speeds. This explains to some extent the calculated higher exit gas temperatures, taking into account the constant coolant temperature of 110°C in the calculation. The heat transfer coefficient of the coolant was determined in a rough estimation assuming hydrodynamically and thermally fully developed flow. Boiling phenomena that might occur in the vicinity of hot walls enhance the heat transfer

coefficient which is another aspect that has to be taken into account when discussing the temperature differences between measurement and calculation.

5. CONCLUSIONS

An unsteady 1-D model of the gas flow in compressor and cylinder head can successfully be applied in designing a cylinder head. The information obtained from the model, referring to the necessary dimensions of plenum chambers and channels in order to meet the specifications, is essential and accurate enough to rely on it in the construction process. However, the comparison between calculation and measurement reveals certain considerable discrepancies. In particular the relatively high temperature mismatch indicates that the neglected heat transfer in the cylinder and in the discharge chamber has an important influence. Considering a transient gas flow in the discharge channel is a must in order to predict the heat transfer in the channel appropriately. The one dimensional approach gives fundamental insights into impacts and consequences of certain measures and delivers the framework for a successful cylinder head design. For a more sophisticated compressor modeling, the heat transfer in cylinder and discharge chamber, as well as the valve motion should be included.

NOMENCLATURE

p	pressure	(Pa)	κ	isentropic coefficient	(-)
T	temperature	(K)	c_p	specific heat at constant pressure	(J/(kg K))
ρ	density	(kg/m ³)	c_v	specific heat constant Volume	(J/(kg K))
v	velocity	(m/s)	λ	heat conductivity	(W/(m K))
n	speed	(1/s)	α	heat transfer coefficient	(W/(m ² K))
φ	effective flow area	(m ²)	τ	shear stress	(Pa)
V	chamber volume	(m ³)	ξ	friction coefficient	(-)
A	channel flow area	(m ²)	Pr	Prandtl number	(-)
L	channel length	(m)	Re	Reynolds number	(-)
P	channel perimeter	(m)	Nu	Nusselt number	(-)
d, D	diameter	(m)	\dot{m}	mass flow	(kg/s)
Δx	spatial discretization	(m)	\dot{w}	specific power consumption	(W/kg)
Δt	time discretization	(s)	\dot{q}	heat flux	(W/m ²)

Subscripts

dis	discharge chamber	suc	suction chamber
$exit$	exit chamber	i, j, k	chambers
w	wall	Nu	Nusselt
ov	overall	amb	ambient
av	average	h	hydraulic

REFERENCES

- Anderson J. D. Jr., 1995, *Computational Fluid Dynamics. The basics with applications*, MacGraw-Hill, 547 p.
 Incropera F. P., DeWitt D. P., 1996, *Fundamentals of Heat and Mass Transfer*, John Wiley & Sons, New York, Chichester, Brisbane, Toronto, Singapore, 879 p.
 Spurk Joseph H., 1997, *Strömungslehre. Einführung in die Theorie der Strömungen*, Springer Verlag Berlin Heidelberg New York, 448 p.
 Verein Deutscher Ingenieure, 1984, *VDI – Wärmeatlas*, VDI – Verlag GmbH Düsseldorf.

ACKNOWLEDGEMENT

Special thanks are due to Olaf Bielmeier and his team at HOERBIGER Kompressortechnik Schongau GmbH, for carrying out the measurements and for the inspiring inputs and discussions.